Development of a Computer Program for Calculating the Transmission-Line Constants of Cables Installed in a Tunnel Taking the Skin and Proximity Effects into Account

Yohei Tanaka, Taku Noda, Yoichi Sekiba, Eiichi Ito, Kazuhiro Misawa, and Takuji Chida

***Abstract*--Accurately calculating the transmission-line constants of overhead lines and underground cables is important for various types of power system simulations. The transmission-line constants of cables installed in a tunnel must be calculated taking the skin and proximity effects into account. This paper presents the development of a computer program for calculating the transmission-line constants of cables installed in a tunnel taking the skin and proximity effects into account. In the developed program, the impedance and admittance are calculated by the MoM-SO and MoM, respectively. The developed program is used to calculate the transmission-line constants of three-phase cables which are closely spaced in a tunnel.**

***Keywords*: cables installed in a tunnel, impedance, admittance, skin effect, proximity effect, electromagnetic transient analysis.**

I. Introduction

ACCURATELY calculating the transmission-line constants of overhead lines and underground cables is important for various types of power system simulations such as electromagnetic transient, power flow, and transient stability simulations. When the phase conductors of a transmission line are widely spaced, the proximity effect can be ignored, and analytical formulas [1]-[5] are available. In [5], the results of the transmission-line constants and propagation characteristics of cables installed in a finite pipe or tunnel directly buried in ground soil is presented. However, cables installed in a tunnel are, in general, closely spaced. Therefore, the current distribution in the cables is influenced by the proximity effect. Considering this point, the transmission-line constants of cables installed in a tunnel must be calculated taking the skin and proximity effects into account.

This paper presents the development of a computer program for calculating the transmission-line constants of cables installed in a tunnel taking the skin and proximity effects into account. In the developed program, the impedance considering the skin and proximity effects is calculated by the MoM-SO (method of moments with a surface admittance operator) [6]-[8] proposed by Patel et al. In the MoM-SO, the current distribution in a conductor is represented by the surface admittance operator [9], and it is discretized and solved by the MoM (method of moments). Differently from the finite-element methods (FEM) [10]-[12] and the conductor subdivision methods [13]-[15] which can also calculate the impedance considering the skin and proximity effects at high frequencies, the MoM-SO allows to replace each conductor by equivalent surface currents and expresses the currents by the Fourier series expansions with respect to the azimuthal angle of that conductor. The FEM and conductor subdivision methods are computationally expensive, since a fine mesh is required in order to precisely represent the skin and proximity effects. On the other hand, the MoM-SO requires only a few Fourier components in order to achieve the same degree of accuracy as those of the FEM and conductor subdivision methods.

In the developed program, the admittance is calculated by the MoM [16]-[18]. In the MoM, conductors and dielectric insulation media are replaced by equivalent surface charges, which are expressed in terms of a few Fourier components in the same way as the MoM-SO. By use of the MoM, the developed program is able to efficiently calculate the admittance considering the proximity effect between metallic sheaths, which are coated with insulating sheaths. In this way, the inhomogeneous media introduced by the insulating sheaths and the surrounding air can be precisely dealt with.

In this paper, the aforementioned methods are described. Then, the developed program is used to calculate the transmission-line constants of three-phase cables which are closely spaced in a tunnel. The calculation results of the frequency responses of the series impedance, modal attenuation constants and modal velocities obtained by the developed program are compared with the results considering the skin effect only (without the proximity effect). The results show that the transmission-line constants of cables installed in a tunnel are influenced by the proximity effect.

II. Numerical Algorithm of the MoM-SO for Calculating the Impedance Matrix

A. Fundamentals of the MoM-SO

In the developed program, the impedance matrix is calculated by the MoM-SO [6]-[8] which is briefly reviewed in this paper. Consider m_1 parallel solid cylindrical conductors

Y. Tanaka and T. Noda are with Energy Innovation Center, CRIEPI (Central Research Institute of Electric Power Industry), 2-6-1, Nagasaka, Yokosuka, Kanagawa 240-0196, Japan (e-mail: {yohei, takunoda}@criepi.denken.or.jp).
Y. Sekiba is with Denryoku Computing Center, 2-11-1 Iwato Kita, Komae, Tokyo 201-0004, Japan (e-mail: sekiba@dcc.co.jp).
E. Ito, K. Misawa, and T. Chida are with Tohoku Electric Power Company,7-2-1, Nakayama, Aoba, Sendai, Miyagi, 981-0952, Japan (e-mail: {ito.eiichi.wu, misawa.kazuhiro.vy, chida.takuji.kd}@tohoku-epco.co.jp).

Paper submitted to the International Conference on Power Systems Transients (IPST2017) in Seoul, Republic of Korea June 26-29, 2017

whose cross section is shown in Fig.1. (a) and also m_2 parallel hollow cylindrical conductors shown in Fig.1. (b). ε_c, μ_c, and σ_c are the permittivity, permeability, and conductivity of the conductor, and ε_0 and μ_0 are the permittivity and permeability of the air. The impedance matrix $\mathbf{Z}$ of $m_c = m_1 + m_2$ parallel conductors satisfies the following equation:

$$\frac{\partial \mathbf{V}}{\partial z} = \mathbf{ZI} \tag{1}$$

where $\mathbf{V}$ and $\mathbf{I}$ are vectors of voltages and currents along the conductors. In the MoM-SO, the conductors are replaced by the surrounding medium and $m_s = m_1 + 2m_2$ equivalent currents shown in Fig. 2. The electric field equation on the pth (p = 1, 2, …, m_s) surface of the conductor is given by

$$E_z^{(p)}\left(\theta_p\right) = -j\omega A_z^{(p)} - \frac{\partial V^{(p)}}{\partial z} \tag{2}$$

where $E_z^{(p)}$ $A_z^{(p)}$, and $V^{(p)}$ are the electric field in z direction, the z-direction component of the vector potential, and the voltage, respectively, on the surface of the conductor. ω is angular frequency, and θ is the azimuthal coordinate. $A_z^{(p)}$ is given as follows:

$$A_z^{(p)} = -\mu_0 \sum_{q=1}^{m_s} \int_0^{2\pi} J_s^{(q)}\left(\theta_q'\right) G\left(\mathbf{r}_p, \mathbf{r}_q\right) a_q d\theta_q' \tag{3}$$

$$G\left(\mathbf{r}, \mathbf{r}'\right) = \frac{1}{2\pi} \ln\left|\mathbf{r} - \mathbf{r}'\right| \tag{4}$$

$$\mathbf{r}_p = \left(x_p + a_p \cos\theta_p,\ y_p + a_p \sin\theta_p\right) \tag{5}$$

where the x_p and y_p are coordinates of the center of the pth conductor. Note that a_p, $E_z^{(p)}$, $A_z^{(p)}$, $J_s^{(p)}$, and $\mathbf{r}_p$ on p = 1, 2, … , m_1 concern the surface of the solid conductor, those on p = m_1 + 1, m_1 + 2, … , $m_1 + m_2 = m_c$ concern the outer surface of the hollow conductor , and those on $p = m_c + 1, m_c + 2, \ldots, m_s$ concern the inner surface of the hollow conductor. $E_z^{(p)}$ and $J_s^{(p)}$ are expressed by the Fourier series expansions

$$E_z^{(p)}\left(\theta_p\right) = \sum_{n=-N_p}^{N_p} E_n^{(p)} e^{jn\theta}$$
$$J_s^{(p)}\left(\theta_p\right) = \frac{1}{2\pi a_p} \sum_{n=-N_p}^{N_p} J_n^{(p)} e^{jn\theta} \tag{6}$$

Using the concept of surface admittance operator [6], [7], [9], the following equations are obtained:

$$\mathbf{J} = \mathbf{YE} \tag{7}$$

$$\mathbf{Y}_s = \begin{bmatrix} \mathbf{Y}^{(1)} & & 0 & & & & & & \\ & \ddots & & & & 0 & & & \\ 0 & & \mathbf{Y}^{(m_1)} & & & & & & \\ & & & \mathbf{Y}_{11}^{(m_1+1)} & \mathbf{Y}_{12}^{(m_1+1)} & & & 0 & \\ & & & \mathbf{Y}_{21}^{(m_1+1)} & \mathbf{Y}_{22}^{(m_1+1)} & & & & \\ & 0 & & & & \ddots & & & \\ & & & & 0 & & \mathbf{Y}_{11}^{(m_c)} & \mathbf{Y}_{12}^{(m_c)} & \\ & & & & & & \mathbf{Y}_{21}^{(m_c)} & \mathbf{Y}_{22}^{(m_c)} & \end{bmatrix} \tag{8}$$

$$\mathbf{E} = \left[E_{-N_1}^{(1)} \cdots E_{N_1}^{(1)} \cdots E_{-N_p}^{(p)} \cdots E_{N_p}^{(p)} \cdots E_{-N_{m_B}}^{(m_s)} \cdots E_{N_{m_B}}^{(m_s)} \right]^T$$
$$\mathbf{J} = \left[J_{-N_1}^{(1)} \cdots J_{N_1}^{(1)} \cdots J_{-N_p}^{(p)} \cdots J_{N_p}^{(p)} \cdots J_{-N_{m_B}}^{(m_s)} \cdots J_{N_{m_B}}^{(m_s)} \right]^T \tag{9}$$

where $\mathbf{Y}^{(p)}$ is the matrix of the surface admittance operator of the solid conductor, and $\mathbf{Y}_{11}^{(p)}$, $\mathbf{Y}_{12}^{(p)}$, $\mathbf{Y}_{21}^{(p)}$, and $\mathbf{Y}_{22}^{(p)}$ are those of the hollow conductor. They are diagonal matrix with entries

$$Y_n^{(p)} = \frac{2\pi}{j\omega}\left[\frac{ka_p \mathcal{J}_{|n|}'\left(ka_p\right)}{\mu \mathcal{J}_{|n|}\left(ka_p\right)} - \frac{k_0 a_p \mathcal{J}_{|n|}'\left(k_0 a_p\right)}{\mu_0 \mathcal{J}_{|n|}\left(k_0 a_p\right)} \right] \tag{10}$$

$$Y_{11,n}^{(p)} = \frac{2\pi}{j\omega}\left[\frac{\chi_n\left(ka_p, ka_{p+m_2}\right)}{\gamma_n\left(ka_p, ka_{p+m_2}\right)\mu_c} - \frac{\chi_n\left(k_0 a_p, k_0 a_{p+m_2}\right)}{\gamma_n\left(k_0 a_p, k_0 a_{p+m_2}\right)\mu_0} \right] \tag{11}$$

$$Y_{12,n}^{(p)} = \frac{2\pi}{j\omega}\left[\frac{\chi_n\left(k_0 a_{p+m_2}, k_0 a_{p+m_2}\right)}{\gamma_n\left(k_0 a_p, k_0 a_{p+m_2}\right)\mu_c} - \frac{\chi_n\left(ka_{p+m_2}, ka_{p+m_2}\right)}{\gamma_n\left(ka_p, ka_{p+m_2}\right)\mu_0} \right] \tag{12}$$

$$Y_{21,n}^{(p)} = \frac{2\pi}{j\omega}\left[\frac{\chi_n\left(k_0 a_p, k_0 a_p\right)}{\gamma_n\left(k_0 a_p, k_0 a_{p+m_2}\right)\mu_c} - \frac{\chi_n\left(ka_p, ka_p\right)}{\gamma_n\left(k\bar{a}_p, ka_{p+m_2}\right)\mu_0} \right] \tag{13}$$

$$Y_{22,n}^{(p)} = \frac{2\pi}{j\omega}\left[\frac{\chi_n\left(ka_{p+m_2}, ka_p\right)}{\gamma_n\left(ka_p, ka_{p+m_2}\right)\mu_c} - \frac{\chi_n\left(k_0 a_{p+m_2}, k_0 a_p\right)}{\gamma_n\left(k_0 a_p, k_0 a_{p+m_2}\right)\mu_0} \right] \tag{14}$$

$$\chi_n\left(\alpha, \beta\right) = \beta\left[\mathcal{H}_{|n|}'\left(\beta\right)\mathcal{K}_{|n|}\left(\alpha\right) - \mathcal{H}_{|n|}\left(\alpha\right)\mathcal{K}_{|n|}'\left(\beta\right) \right] \tag{15}$$

$$\gamma_n\left(\alpha, \beta\right) = \mathcal{H}_{|n|}\left(\alpha\right)\mathcal{K}_{|n|}\left(\beta\right) - \mathcal{H}_{|n|}\left(\beta\right)\mathcal{K}_{|n|}\left(\alpha\right) \tag{16}$$

where

$$k = \sqrt{\omega\mu_c\left(\omega\varepsilon_c - j\sigma_c\right)}, \quad k_0 = \omega\sqrt{\mu_0\varepsilon_0}\ . \tag{17}$$

$\mathcal{J}_n$ is the Bessel function of the nth order of the first kind, $\mathcal{H}_n$ is the Hankel function of the nth order of the first kind, and $\mathcal{K}_n$ is the Hankel function of the nth order of the second kind. $\mathbf{E}$ and $\mathbf{J}$ have a size N, which is given by

$$N = \sum_{p=1}^{m_s}\left(2N_p + 1\right) \tag{18}$$

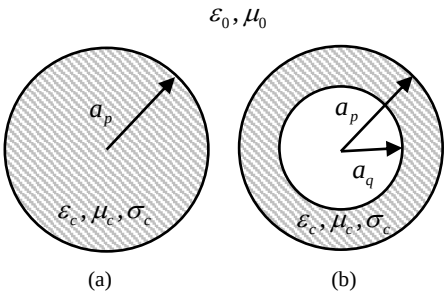

Fig. 1. (a) Solid cylindrical conductor (b) Hollow cylindrical conductor.

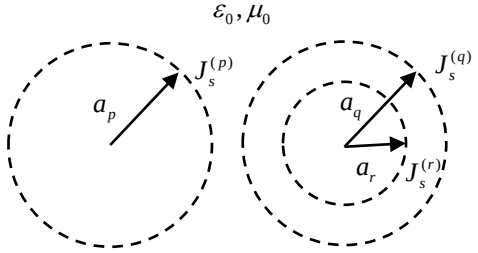

Fig. 2. Solid and hollow conductors which are replaced by the surrounding medium and equivalent currents.

The equation (2) is solved numerically by the MoM using the Fourier series expansions, and the following algebraic equation can be obtained

$$\mathbf{E} = j\omega\mu_0\mathbf{G}\mathbf{J} + \mathbf{U}\mathbf{Z}\mathbf{U}^T\mathbf{J} \tag{19}$$

where the matrix **G** is obtained by the discretization of Green's function and given by

$$\mathbf{G} = \begin{bmatrix} \mathbf{G}^{(1,1)} & \cdots & \mathbf{G}^{(1,m_s)} \\ \vdots & \ddots & \vdots \\ \mathbf{G}^{(m_s,1)} & \cdots & \mathbf{G}^{(m_s,m_s)} \end{bmatrix}$$

$$\mathbf{G}^{(p,q)} = \begin{bmatrix} G^{(p,q)}_{-N_p,-N_q} & \cdots & G^{(p,q)}_{-N_p,N_q} \\ \vdots & \ddots & \vdots \\ G^{(p,q)}_{N_p,-N_q} & \cdots & G^{(p,q)}_{N_p,N_q} \end{bmatrix} \tag{20}$$

$$G^{(p,q)}_{n',n} = \frac{1}{(2\pi)^2}\int_0^{2\pi}\int_0^{2\pi} G\left(\mathbf{r}_p(\theta),\mathbf{r}_q(\theta')\right)e^{j(n\theta'-n'\theta)}d\theta d\theta' \tag{21}$$

The matrix **U** is an N by m_c matrix. In the pth column, if the pth conductor is solid (p = 1, 2, …, m_1), the row corresponding to the position of $J_0^{(p)}$ in (9) is "1". If the pth conductor is hollow ($p = m_1 + 1, m_1 + 2, \ldots, m_c$), the row corresponding to the position of $J_0^{(p)}$ and $J_0^{(p+m_2)}$ in (9) is "1". All other entries of **U** are zeros. From (7) and (19), the impedance matrix **Z** is given by

$$\mathbf{Z} = \left[\mathbf{U}^T\left(\mathbf{1} - j\omega\mu_0\mathbf{Y}_s\mathbf{G}\right)^{-1}\mathbf{Y}_s\mathbf{U}\right]^{-1} \tag{22}$$

B. Representation of a tunnel [8]

Fig. 3 shows the cross section of a solid conductor and a hollow conductor installed in a tunnel which is buried in ground soil. In the MoM-SO, the conductors and the surface of the tunnel are replaced by the surrounding medium and equivalent currents shown in Fig. 4. If the m_c conductors explained in Section II-A are installed in the tunnel, the electric field equation (2) is rewritten as follows:

$$E_z^{(p)} = -j\omega\hat{A}_z^{(p)} - j\omega A_z^{(p)} - \frac{\partial V^{(p)}}{\partial z} \tag{23}$$

where vector potential $\hat{A}_z^{(p)}$ is given by the equivalent current $\hat{J}_s$ and the solution of the Helmholtz equation. The integral equation (23) is solved numerically by the MoM using the Fourier series expansions and following algebraic equation can be obtained

$$\mathbf{E} = j\omega\mu_0\left(-\mathbf{H}\mathbf{C} + \mathbf{G}\mathbf{J}\right) + \mathbf{U}\mathbf{Z}\mathbf{U}^T\mathbf{J} \tag{24}$$

In (24), the matrix **H** and **C** are described in detail in [8]. From (7) and (24), the impedance matrix **Z** of the conductors in the tunnel is given by

$$\mathbf{Z} = \left[\mathbf{U}^T\left(\mathbf{1} - j\omega\mu_0\mathbf{Y}_s\mathbf{\Psi}\right)^{-1}\mathbf{Y}_s\mathbf{U}\right]^{-1} \tag{25}$$

$$\mathbf{\Psi} = \mathbf{H}\mathbf{C} + \mu_0\mathbf{G}_c \tag{26}$$

III. Numerical Algorithm of the MoM for Calculating the Admittance Matrix

The admittance matrix between metallic sheaths considering the proximity effect is calculated by the MoM [16]-[18] which is briefly reviewed in this paper. Fig. 5 shows a solid conductor which is coated with an insulating sheath whose permittivity is ε_p. Note that, since the charge on the outer surface of the metallic sheath dose not interfere with the charges on inner surface of the metallic sheath and on the surface of the core, the metallic sheath shown in Fig. 5 is represented by the solid conductor. The capacitance matrix **C** of m parallel conductors whose cross section is shown Fig.5 is obtained from the inverse of the potential coefficient matrix **P**. **P** satisfies the following equation:

$$\mathbf{V} = \mathbf{P}\mathbf{Q}_f \tag{27}$$

where **V** is a vector of voltages, and $\mathbf{Q}_f$ is a vector of total free charges on the surface of the conductors. In the MoM, the pth conductor and insulating sheath are replaced by the surrounding medium and equivalent charges Q_p and Q_p^*, respectively, shown in Fig. 6. Q_p is the total charge on the surface of the pth conductor, and Q_p^* is the total bound charge on the surface of the pth insulating sheath. The total free charge of the pth conductor is obtained from Q_p and Q_p^* on two surfaces as

$$Q_{fp} = Q_p + Q_p^* \tag{28}$$

The potential at an arbitrary point from the center of the pth conductor is given by

$$\phi^{(p)}(\rho,\theta) = -\frac{1}{\varepsilon_0}\sum_{q=1}^{m}\left[\int_0^{2\pi}\sigma^{(q)}(\theta')G\left(\mathbf{r}_p(\rho,\theta),\mathbf{r}_q(a_q,\theta')\right)a_q d\theta' + \int_0^{2\pi}\sigma^{*(q)}(\theta')G\left(\mathbf{r}_p(\rho,\theta),\mathbf{r}_q(b_q,\theta')\right)b_q d\theta'\right] \tag{29}$$

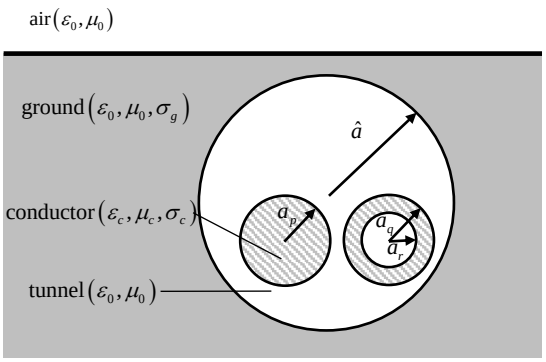

Fig. 3.Solid and hollow conductors installed in a tunnel.

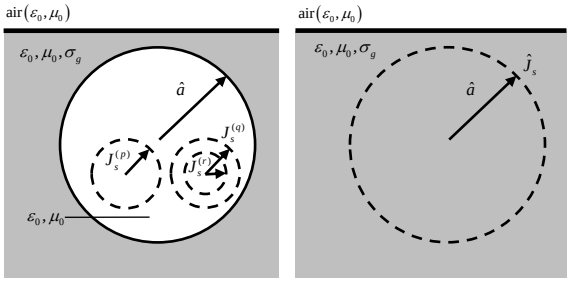

(a) (b)

Fig. 4. (a) Solid and hollow conductors and (b) surface of the tunnel which are replaced by the surrounding medium and equivalent currents.

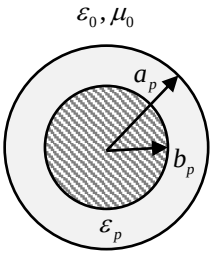

Fig. 5. Solid conductor which is coated with insulating sheath.

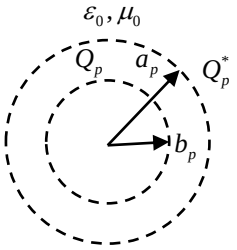

Fig. 6. Solid conductor and insulating sheath which are replaced by the surrounding medium and equivalent charges.

$$G(\mathbf{r},\mathbf{r}') = \frac{1}{2\pi}\ln|\mathbf{r}-\mathbf{r}'| \tag{30}$$

$$\mathbf{r}_p(\rho,\theta) = \left(x_p + \rho\cos\theta_p,\ y_p + \rho\sin\theta_p\right) \tag{31}$$

where $\sigma^{(p)}$ and $\sigma^{*(p)}$ are charge distribution on surface of the pth conductor and insulating sheath. The voltage of pth conductor is given by:

$$\begin{aligned} V_p = -\frac{1}{\varepsilon_0}\sum_{q=1}^{m}\Bigg[&\int_0^{2\pi}\sigma^{(q)}(\theta')G\left(\mathbf{r}_p(a_p,\theta),\mathbf{r}_q(a_q,\theta')\right)a_q d\theta' \\ &+\int_0^{2\pi}\sigma^{*(q)}(\theta')G\left(\mathbf{r}_p(a_p,\theta),\mathbf{r}_q(b_q,\theta')\right)b_q d\theta'\Bigg] \end{aligned} \tag{32}$$

Substituting (27) into (32) gives the following equation is obtained:

$$\begin{aligned} \sum_{q=1}^{m}P_{pq}Q_q = -\frac{1}{\varepsilon_0}\sum_{q=1}^{m}\Bigg[&\int_0^{2\pi}\sigma^{(q)}(\theta')G\left(\mathbf{r}(a_p,\theta),\mathbf{r}(a_q,\theta')\right)a_q d\theta' \\ &+\int_0^{2\pi}\sigma^{*(q)}(\theta')G\left(\mathbf{r}(a_p,\theta),\mathbf{r}(b_q,\theta')\right)b_q d\theta'\Bigg] \end{aligned} \tag{33}$$

Since the electric flux density is must be continuous on interfaces between the insulating sheaths and the air, the following equations are obtained:

$$\begin{aligned} &\varepsilon_p E_{in}^{(p)} - \varepsilon_0 E_{out}^{(p)} = 0 \\ &E_{in}^{(p)} = -\left[\frac{\partial\phi_{in}^{(p)}}{\partial\rho}\right]_{\rho=b_p} \quad E_{out}^{(p)} = -\left[\frac{\partial\phi_{out}^{(p)}}{\partial\rho}\right]_{\rho=b_p} \end{aligned} \tag{34}$$

where ϕ_{in} is the potential on $b_p < \rho$,and ϕ_{out} is the potential on $b_p \geq \rho$. In the MoM, $\sigma^{(p)}$, $\sigma^{*(p)}$, and $\phi^{(p)}$ are expressed by the Fourier series expansions in the same way as the MoM-SO. They are given as follows:

$$\begin{aligned} \sigma^{(p)}(\theta) &= \frac{1}{2\pi a_p}\sum_{n=-N_p}^{N_p}\sigma_n^{(p)}e^{jn\theta} \\ \sigma^{*(p)}(\theta) &= \frac{1}{2\pi b_p}\sum_{n=-N_p}^{N_p}\sigma_n^{*(p)}e^{jn\theta} \\ \phi^{(p)}(\theta) &= \sum_{n=-N_p}^{N_p}\phi_n^{p}e^{jn\theta} \end{aligned} \tag{35}$$

From (33), (34), and (35), the following algebraic equation is given by

$$\mathbf{UPQ}_f = -\frac{1}{\varepsilon_0}\begin{bmatrix}\mathbf{G} & \mathbf{G}^* \\ \tilde{\mathbf{G}} & \tilde{\mathbf{G}}^*\end{bmatrix}\begin{bmatrix}\boldsymbol{\sigma} \\ \boldsymbol{\sigma}^*\end{bmatrix} \tag{36}$$

$$\begin{aligned} \boldsymbol{\sigma} &= \left[\sigma_{-N_1}^{(1)}\cdots\sigma_{N_1}^{(1)}\cdots\sigma_{-N_p}^{(p)}\cdots\sigma_{N_p}^{(p)}\cdots\sigma_{-N_m}^{(m)}\cdots\sigma_{N_m}^{(m)}\right]^T \\ \boldsymbol{\sigma}^* &= \left[\sigma_{-N_1}^{*(1)}\cdots\sigma_{N_1}^{*(1)}\cdots\sigma_{-N_p}^{*(p)}\cdots\sigma_{N_p}^{*(p)}\cdots\sigma_{-N_m}^{*(m)}\cdots\sigma_{N_m}^{*(m)}\right]^T \end{aligned} \tag{37}$$

where $\boldsymbol{\sigma}$ and $\boldsymbol{\sigma}*$ are the vectors of the Fourier components. They have a size N which is given by

$$N = \sum_{p=1}^{n}\left(2N_p + 1\right) \tag{38}$$

The matrix $\mathbf{U}$ is an $2N$ by m matrix. In the pth column, the row corresponding to the position of $\sigma_0^{(p)}$ and $\sigma_0^{*(p)}$ in (37) is "1". All other entries of $\mathbf{U}$ are zeros. The Green's function matrix $\mathbf{G}$, $\mathbf{G}^*$, $\tilde{\mathbf{G}}$ and $\tilde{\mathbf{G}}^*$ are given by

$$\mathbf{G} = \begin{bmatrix} G^{(1,1)} & \cdots & G^{(1,m)} \\ \vdots & \ddots & \vdots \\ G^{(m,1)} & \cdots & G^{(m,m)} \end{bmatrix}_{\rho=a_p} \tag{39}$$

$$\mathbf{G}^* = \begin{bmatrix} G^{*(1,1)} & \cdots & G^{*(1,m)} \\ \vdots & \ddots & \vdots \\ G^{*(m,1)} & \cdots & G^{*(m,m)} \end{bmatrix}_{\rho=a_p} \tag{40}$$

$$\tilde{\mathbf{G}} = \frac{\partial}{\partial\rho}\left(-\varepsilon_p\mathbf{G}\big|_{\rho<b_p} + \varepsilon_0\mathbf{G}\big|_{\rho\geq b_p}\right)\Big|_{\rho=b_p} \tag{41}$$

$$\tilde{\mathbf{G}}^* = \frac{\partial}{\partial\rho}\left(-\varepsilon_p\mathbf{G}^*\big|_{\rho<b_p} + \varepsilon_0\mathbf{G}^*\big|_{\rho\geq b_p}\right)\Big|_{\rho=b_p} \tag{42}$$

$$G_{n',n}^{(p,q)} = \frac{1}{(2\pi)^2}\int_0^{2\pi}\int_0^{2\pi}G\left(\mathbf{r}(\rho,\theta),\mathbf{r}(a_q,\theta')\right)e^{j(n\theta'-n'\theta)}d\theta d\theta' \tag{43}$$

$$G_{n',n}^{(p,q^*)} = \frac{1}{(2\pi)^2}\int_0^{2\pi}\int_0^{2\pi}G\left(\mathbf{r}(\rho,\theta),\mathbf{r}(b_q,\theta')\right)e^{j(n\theta'-n'\theta)}d\theta d\theta' \tag{44}$$

From (36), the capacitance matrix $\mathbf{C}$ can be obtained:

$$\mathbf{C} = \mathbf{P}^{-1} = -\varepsilon_0\mathbf{U}^T\begin{bmatrix}\mathbf{G} & \mathbf{G}^* \\ \tilde{\mathbf{G}} & \tilde{\mathbf{G}}^*\end{bmatrix}^{-1}\mathbf{U} \tag{45}$$

Finally, the admittance matrix $\mathbf{Y}$ is given by

$$\mathbf{Y} = j\omega\mathbf{C}\,. \tag{46}$$

Note that the admittance matrix considering a tunnel can be obtained by replacing the surface of the tunnel with the equivalent charge which is expressed by the Fourier series expansions.

IV. Numerical Results

In the developed program, the transmission-line constants of cables installed in a tunnel are obtained by the following steps: (i) Reading the cable arrangement data; (ii) Calculating the impedance and admittance; (iii) Calculating the modal

constants from the impedance and admittance. Fig. 7 shows three-phase cables installed in a tunnel which is buried in ground soil. The impedance and admittance are calculated by the developed program with the truncation order $N_p = 0$ and $N_p = 8$. When the truncation order is set to $N_p = 0$, the calculation results considering the skin effect only (without the proximity effect) can be obtained.

Fig. 8 shows the frequency response of the self-resistance and self-inductance of phase *a*, and Fig. 9 shows those of the positive-sequence resistance and inductance (the metallic sheaths are opened). Note that the positive-sequence impedance is defined as the ratio of positive-sequence voltages and currents. The current distribution considering the skin and proximity effects ($N_p = 8$) is smaller than that considering the skin effect only ($N_p = 0$). Thus, there are the deviation between the results with $N_p = 8$ and those with $N_p = 0$. Note that, since the ground-return impedance, which is larger than the conductor-internal impedance, is hardly influenced by the proximity effect, the deviation in Fig. 8 is small.

Fig. 10 shows the frequency responses of the modal attenuation constants and modal velocities. The admittance is independent on frequency and is strongly influenced by the proximity effect, since the charges are distributed on the outer surface of the metallic sheaths. Therefore, the modal constants shown in Fig. 10 are influenced by the proximity effect even in low frequency region.

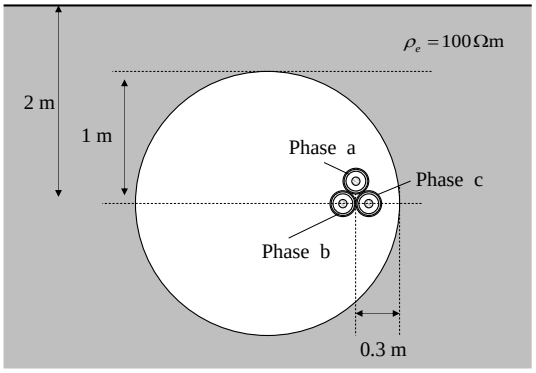

(a) Arrangement.

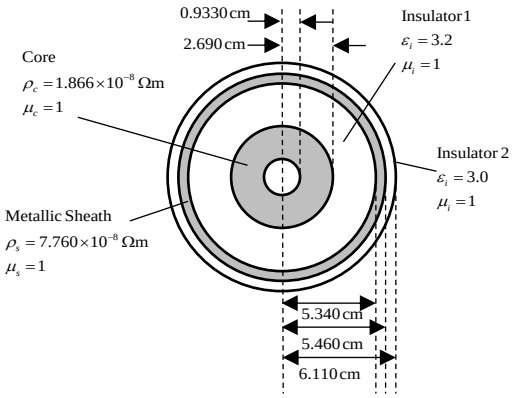

(b) Cross section of each cable.

Fig. 7. Three–phase cables installed in a tunnel.

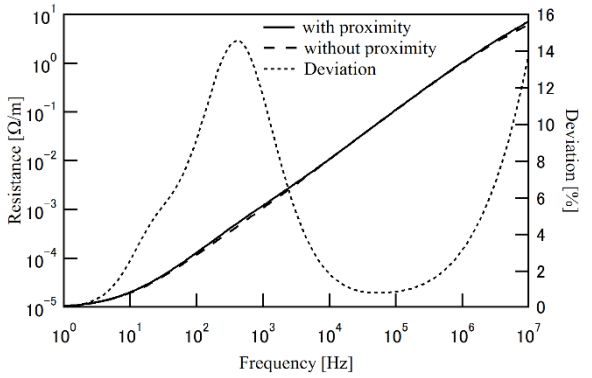

(a) Resistance of the core.

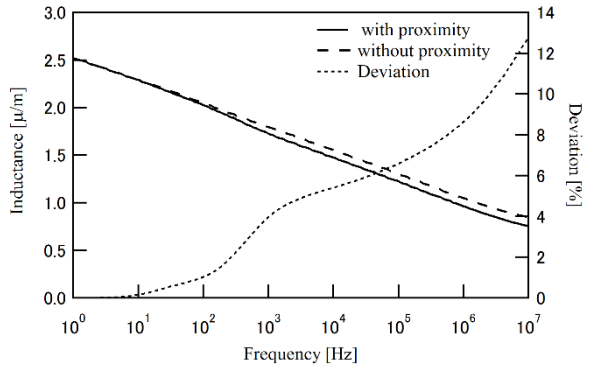

(b) Inductance of the core.

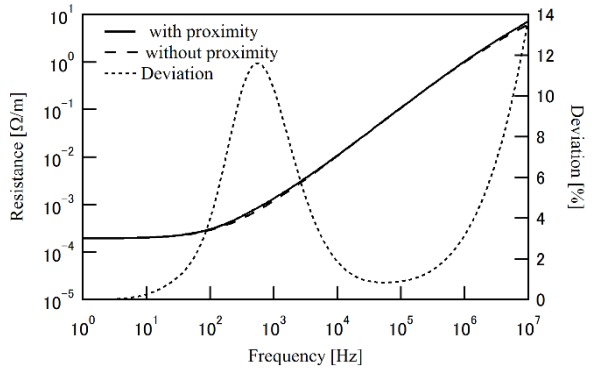

(c) Resistance of the sheath.

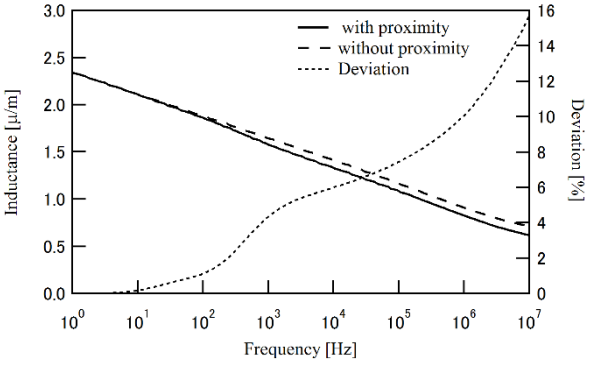

(d) Inductance of the sheath

Fig. 8. Calculated results of the self-impedance.

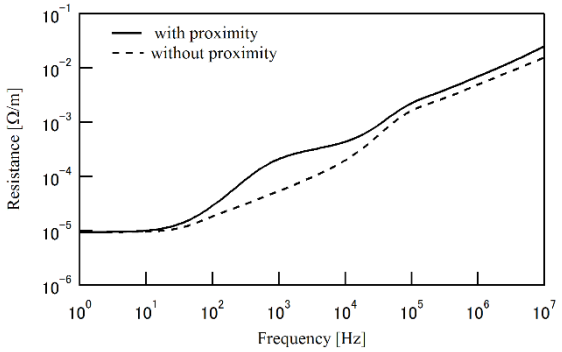

(a) Positive-sequence resistance.

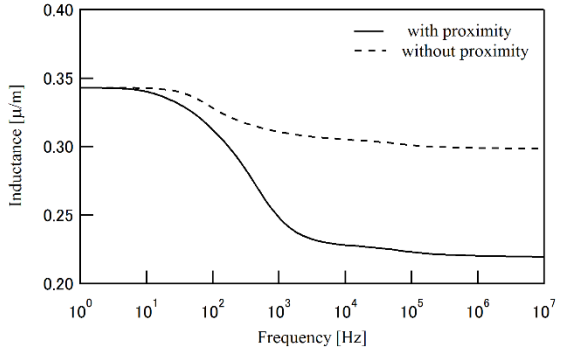

(b) Positive-sequence inductance.

Fig. 9. Calculated results of positive-sequence impedance.

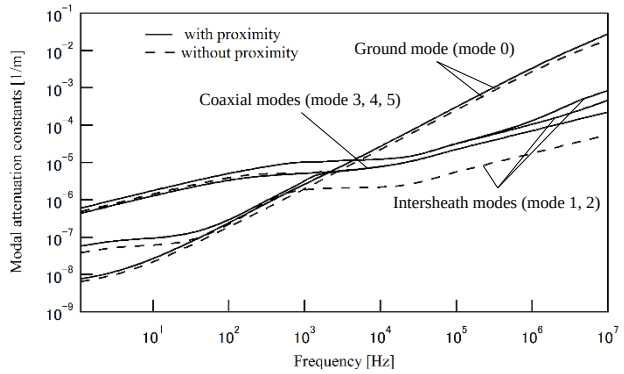

(a) Modal attenuation constants

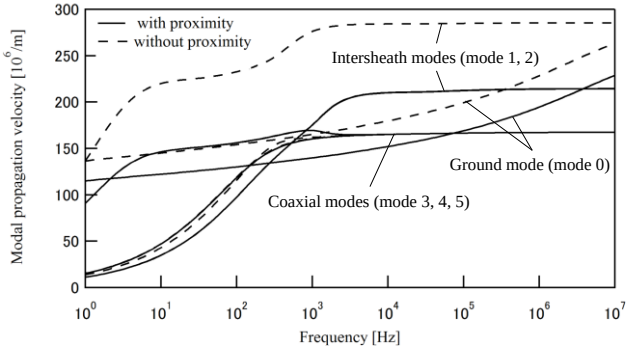

(b) Modal velocities

Fig. 10. Calculated results of modal constants.

V. Conclusion

This paper presents the development of a computer program for calculating the transmission-line constants of cables installed in a tunnel taking the skin and proximity effects into account. The developed program is used to calculate the transmission-line constants of three-phase cables which are closely spaced in a tunnel. The results show that the transmission-line constants of cables installed in a tunnel are influenced by the proximity effect.

VI. References

[1] J. R. Carson, "Wave propagation in overhead wires with ground return," *Bell System Technical Journal*, vol. 5, pp. 539-554, 1926.

[2] F. Pollaczek, "Über das Feld einer unendlich langen wechselstrom-durchflossenen Einfachleitung," *E. N. T.*, Band 3 (Heft 9), pp. 339-360, 1926.

[3] F. Pollaczek, "Über die Induktionswirkungen einer Wechselstrom-einfachleitung," *E. N. T.*, Band 4 (Heft 1), pp. 18-30, 1927.

[4] S. A. Schelkunoff, "The electromagnetic theory of coaxial transmission line and cylindrical shields," *Bell System Technical Journal*, vol. 13, pp. 532-579, 1934.

[5] N. Amekawa, N. Nagaoka, and A. Ametani, "Impedance derivation and wave propagation characteristics of pipe-enclosed and tunnel-installed cables," *IEEE Trans., Power Del*, vol. 19, no. 1, pp. 380-386, 2004.

[6] U. R. Patel, B, Gustavesen, and P. Triverio, "An equivelnt surface current approach for the computation of the series impedance of power cables eith inclusion of skin and proximity effects," *IEEE Trans., Power Del*, vol. 28, no. 4, pp. 2474-2482, 2013.

[7] U. R. Patel, B, Gustavesen, and P. Triverio, "Proximity-aware calculation of cables series impedance for systems of solid and hollow conductors," *IEEE Trans., Power Del*, vol. 29, no. 5, pp. 2101-2109, Oct, 2014.

[8] U. R. Patel and P. Triverio, "MoM-SO: a complete method for computing the impedance of cables systems including skin, proximity, and ground return effects," *IEEE Trans., Power Del*, vol. 30, no. 5, pp. 2110-2118, Dec, 2015.

[9] D.D. Zutter and L. Knockaert, "Skin effect modeling based on a differential surace admittance operator," *IEEE Trans., Microw. Theory Tech.*, vol. 53, no. 8, pp. 2526-2538, Aug, 2005.

[10] R. Lucas and S. Talukdar, "Advances in finite element techniques for calculating cable resistances and inductances," *IEEE Trans., Power App. Syst.*, vol. PAS-97, no. 3, pp. 875-883, May, 1978.

[11] S. Cristina and M. Feliziani, "A finite element technique for multiconductor cable parameters," *IEEE Trans. Magn.*, vol. 25, no. 4, pp. 2986-2988, Jul, 1989.

[12] B. Gustavsen, A. Bruaset, J. Bremnes, and A. Hassel, "A finite element approach for calculating electrical parameters of umbilical cables," *IEEE Trans., Power Del*, vol. 24, no. 4, pp. 2375-2384, Oct, 2009.

[13] P. de. Arizon and H. W. Dommel, "Computation of cable impedances based on subdivision of conductors," *IEEE Trans., Power Del*, vol. 2, no. 1, pp. 21-27, Jan, 1987.

[14] D. Zhou and J. R. Marti, "Skin effect calculations in pipe-type cables using a linear current subconductor technique," *IEEE Trans., Power Del*, vol. 9, no. 1, pp. 598-604, Jan, 2008.

[15] M. Miki and T. Noda, "An improvement of a conductor subdivision method for calculating the series impedance matrix of a transmission line considering the skin and proximity effects," *IEE Japan*, vol. 128-B, no. 1, pp. 254-262, Jan, 2008 (in Japanese).

[16] J. C. Clements, C. R. Paul, and A. T. Adams, "Computation of the capacitance matrix for systems of dielectric-coated cylindrical conductors," *IEEE Trans. EMC.*, vol. 17, no. 4, pp. 238-248, Nov, 1975.

[17] J. S. Savage and W. T. Smith, "Capacitance calculations for cable harnesses using the method of moments," *IEEE Trans. EMC.*, vol. 37, no. 1, pp. 131-137, Feb, 1995.

[18] J. B. Faria and M. G. Neves "Accurate evaluation of indoor triplex cable capacitances taking conductor proximity effects into account," *IEEE Trans., Power Del*, vol. 21, no. 3, pp. 1238-1244, Jul, 2006.